Pergamon

Tetrahedron 58 (2002) 6825–6835

TETRAHEDRON

Isolation and identification of antifungal polyesters from the marine fungus *Hypoxylon oceanicum* LL-15G256

Gerhard Schlingmann,* Lisa Milne† and G. T. Carter

Natural Products Chemistry, Chemical Sciences, Wyeth Research, 401 North Middletown Road, Pearl River, NY 10965, USA

Received 23 May 2002; revised 26 June 2002; accepted 1 July 2002

Abstract—Cultures of the marine fungus *Hypoxylon oceanicum* (LL-15G256) were found to have potent antifungal activity in assays designed to detect inhibitors of fungal cell wall biosynthesis. Bio-activity guided isolation provided the macrocyclic polyesters 15G256α (**1**), 15G256α-1 (**2**) and 15G256β (**3**) that were partially responsible for the antifungal activity. In addition, fermentation beers contained a series of related, but unreported metabolites designated 15G256ι (**4**), 15G256ω (**5**), 15G256ο (**6**), 15G256α-2 (**7**), 15G256β-2 (**8**), 15G256ν (**9**) and 15G256π (**10**). Their isolation, characterization and structures are described here and a biosynthetic sequence is proposed.

1. Introduction

In our search for new antifungal metabolites[1] we investigated the marine fungus *Hypoxylon oceanicum* (culture LL-15G256) and subsequently isolated the antifungal lipodepsipeptides 15G256γ, 15G256δ and 15G256ε.[1a] During the investigation we discovered that this culture not only produced the lipodepsipeptides but also macrocyclic polyesters (lactides), such as 15G256α (**1**), 15G256α-1 (**2**), and 15G256β (**3**) that were equally potent as antifungals. Thorough HPLC analysis of fermentation extracts revealed that in addition to these lactides, a series of related polyesters was co-produced. The majority of these polyesters has now been purified and characterized. These compounds can be grouped according to their polarity as follows: group I comprise the relatively hydrophobic components that elute from silica gel with ethyl acetate, whereas group II include the more polar components that require the use of methanol for elution from silica gel. Besides the known 15G256α (**1**), 15G256α-1 (**2**), and 15G256β (**3**), group I contained the new macrocyclic polyesters 15G256ι (**4**) and 15G256ω (**5**) (see Fig. 1), as well as very small amounts of the linear butyrolactone-polyester 15G256ο (**6**). Among the constituents of group II we found the known 3-hydroxybutyric acid (**17**) and (*R*)-6-hydroxymellein (**16**), supposedly the building blocks of the polyesters, as well as the new components 15G256α-2 (**7**), 15G256β-2 (**8**), 15G256ν (**9**), and 15G256π (**10**) (see Fig. 2).

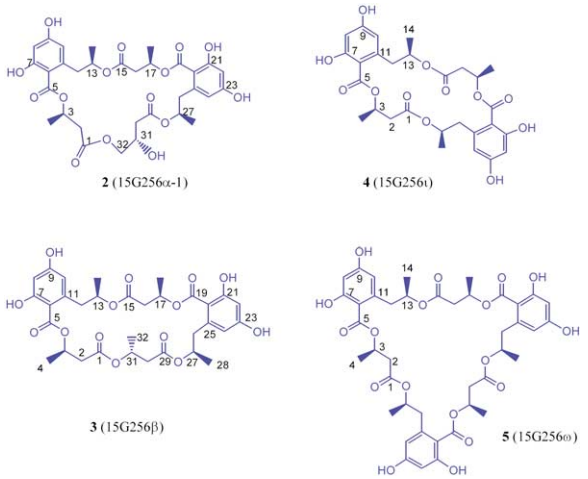

Figure 1. Structures of the 15G256 macrocyclic polyesters (lactides) **2**(α-1), **3**(β), **4**(ι), and **5**(ω).

2. Results and discussion

2.1. Isolation

The 15G256 polyesters were readily isolated from fermentation broths by either solvent extraction or resin adsorption. Typically, harvested fermentation broth was centrifuged or filtrated to separate the supernatant from the pellet. The polyesters retained with the pellet were extracted by slurrying with 85% acetone. Filtration of the slurry and subsequent concentration of the filtrate yielded an aqueous mixture from which the polyesters were recovered by extraction with ethyl acetate. The polyesters contained in the supernatant were either recovered by extraction with

Keywords: marine fungus; antifungal metabolites; macrolides; lactide biosynthesis; polyesters; isolation; natural product; circular dichroism; NMR.

* Corresponding author. Tel.: +1-845-602-4390; fax: +1-945-602-5687; e-mail: schling@wyeth.com

† Present address: University of California, Los Angeles, CA 90024, USA.

0040–4020/02/$ - see front matter
PII: S0040-4020(02)00746-9

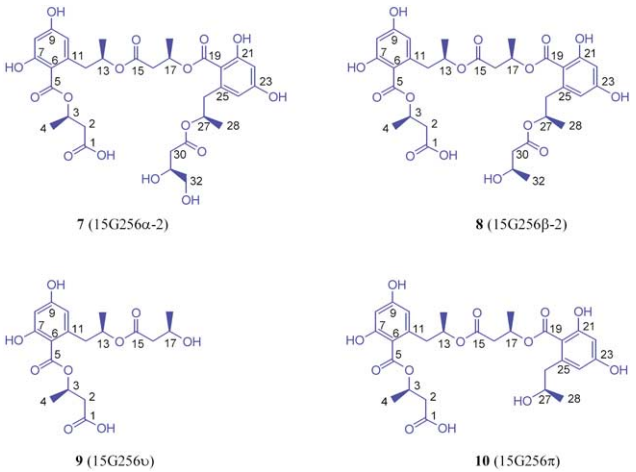

Figure 2. Structures of the 15G256 linear polyesters **7**(α-2), **8**(β-2), **9**(*ν*), and **10**(π).

ethyl acetate or, alternatively, by adsorption on Amberchrom CG 161dm and subsequent elution with 90% MeOH. Evaporation of the organic solvent extracts produced dark-brown, viscous oils from which single polyester components were obtained by silica gel and reverse phase column chromatographies.

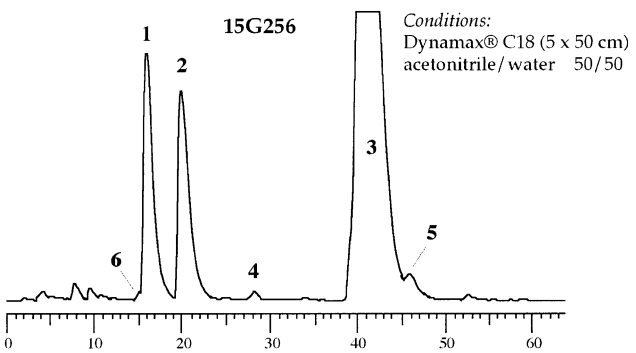

Figure 3. Preparative HPLC of the 15G256 macrocyclic polyesters (lactides).

The lactides (**1**–**3**) are usually produced in substantial quantities and represent the bulk of the polylactone components. They are easily separated from each other and purified by preparative reverse phase chromatography (Fig. 3). Purification of these compounds by chromatography on silica gel or Amberchrom CG 161dm can be used as an alternative method, although the order of elution may change depending on the method employed.

On silica gel, using increasing concentrations of ethyl acetate (10, 25, 50, and 100%) in methylene chloride, **3** elutes first followed by **4**, **5** and **6**. Next is **2** which elutes just before **1**. Compounds **9**, **10**, **7** and **8** (eluting in this order) are usually recovered together from the silica gel column by washing with methanol. These latter components are best purified and separated from each other by reverse phase chromatography employing conditions as outlined in Fig. 4.

On Amberchrom CG 161dm using aqueous methanol concentrations from 70 to 90%, the polyesters are eluted in the following order, **7**(α-2), **9**(*ν*), **10**(π), **8**(β-2), **1**(α), **2**(α-1), **3**(β) together with **4**(ι), and lastly, **5**(ω).

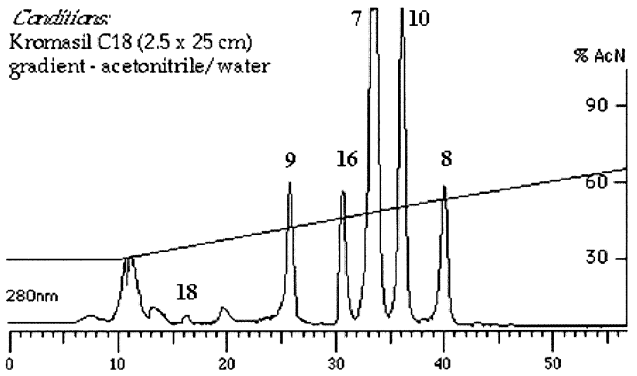

Figure 4. Preparative HPLC of the linear polyesters **9**(*ν*), **7**(α-2), **10**(π) and **8**(β-2).

2.2. Structure elucidation

Structure assignments of the 15G256 polyesters are based on the interpretation of spectroscopic data, especially those from MS and NMR analysis. The structure of **1**(α), isolated first, was recognized as a macrocyclic pentalactone inferred from a set of five proton/carbon NMR signals at 5.53/70.1, 5.25/72.7, 5.50/70.3, 5.03/73.9 and 5.01/73.4 ppm. In addition, the LC/ESIMS spectrum revealed a dominant $[M+H]^+$-ion peak at m/z=663 and virtually no fragment ions, suggesting that the molecule was cyclic. A search for natural products with matching properties uncovered the identity of **1**(α) with BK233-A[2] also known as NG-012.[3] With the structure of **1**(α) known and the UV spectra of **1**–**3** virtually identical, the structures of **2**(α-1) and **3**(β) were readily deduced from their NMR data. The difference between **3** and **1** or **2** is indicated by the molecular weight of **3** (646.6 vs. 662.6) that suggested the lack of an oxygen atom. As a new NMR signals at 1.24 (d) and 19.91 ppm (q) replaced the signals for the only hydroxymethylene group found in **1** or **2** (no DEPT signal for a CH_2-group between 60 and 70 ppm), it was apparent that **3**(β) contained five methyl groups and its structure was therefore consistent with the macrocyclic pentalactone shown in Fig. 1. A review of the literature data revealed that **3**(β) is identical with BK233-C[2] and BE-26263.[4] Published data for orbuticin[5] suggest that this compound is also identical with **3**(β).

A thorough NMR analysis of **2**(α-1) uncovered that this compound is a regio-isomer of **1**(α) and identical in every respect with BK233-B.[2] (Although the published NMR data of BK233-B refer to acetone solutions, they agree well with our data for **2**(α-1) obtained on MeOH-d_4 solutions). The assignments, shown in Fig. 5, are based on HMBC as well as chemical shift values, and demonstrate the difference between the ester linkages in **1**(α) and **2**(α-1) where ring closure occurred via an unexpected γ-hydroxyester linkage

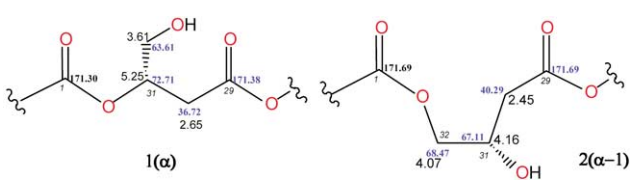

Figure 5. NMR chemical shift assignments demonstrate the different linkages in **1** vs **2**.

rather than the usual β-hydroxyester bond found in **1**(α) and **3**(β). It is noteworthy that precedence for this type of one bond 'ring enlargement' has also been observed in the lipodepsipeptide series with compound15G256δ[1b] where the widening of the ring also occurred via the hydroxylation of a methyl group. As the NMR data recorded for **2**(α-1) agree well with those published for NG-011, the identity of these compounds is indicated, suggesting that NG-011[3] is the regio-isomer of NG-012 or **1** (15G256α) rather than its stereo-isomer as claimed.

The structure of 15G256ι (**4**) was determined as follows. A molecular formula of $C_{28}H_{32}O_{12}$ was established by HRFAB mass spectrometry ($[M+Na]^+$ found: 583.1784, calcd: 583.1777). However, the ^1H and ^{13}C NMR spectra revealed signals and correlations for only 14 carbon and 16 hydrogen atoms indicating one β-hydroxybutyrate and one 3,5-dihydroxy-7-(β-hydroxypropyl)-benzoate group. Consequently, **4**(ι) had to consist of two units each and these moieties were arranged symmetrically as illustrated in Fig. 1.

Similarly, the molecular formula of 15G256ω (**5**) is based on its molecular ion $[M+H]^+=m/z$ 841.29114, calculated for $C_{42}H_{49}O_{18}$=841.29134 (Δ=−0.2 mmu) as determined by HRFTMS mass spectrometry, invoking a molecular formula of $C_{42}H_{48}O_{18}$. The ^1H and ^{13}C NMR signals of **5** were remarkably similar to those of **4**. Again, the ^1H and ^{13}C NMR spectra of **5**(ω) accounted for only 14 carbon and 16 hydrogen atoms derived from one β-hydroxylbutyrate ester linked to one 3,5-dihydroxy-7-(β-hydroxypropyl)-benzoate group. While only the signals for the protons in position 2 (H-2a,b) in **5** appear as dd at 2.63 and 2.77 ppm, the signals for the same protons are degenerate in **4** and appear as a single doublet at 2.74 ppm (H-2a,b, ^3J=6.1 Hz). However, the protons (H-12a,b) for both, **4** and **5**, appear as dd, and resonate at 3.18 ppm (12a, ^3J=8.1 Hz, ^2J=13.8 Hz, *trans* to Me) and 3.00 ppm (12b, ^3J=5.7 Hz, ^2J=13.8 Hz, *cis* to Me) for **5** and at 3.51 ppm (12a, ^3J=6.5 Hz, ^2J=13.2 Hz, *trans* to Me) and 2.83 ppm (12b, ^3J=8.4 Hz, ^2J=13.2 Hz, *cis* to Me) for **4**, respectively. Although the NMR spectra of **5** suggested the presence of only two units, its molecular weight required a compound three times larger in size. Given the molecular formula, **5** must exist in the form of a symmetric trimer as depicted in Fig. 1. Molecular modeling suggested that **5** assumes the shape of 'propeller' where the benzoate moieties are slightly tilted out of plane. The occurrence of a macrocyclic natural product with C_3-symmetry is a relatively rare event, but there is precedence in the depsipeptide beauvericin.[6]

Although 15G256ο (**6**) is indistinguishable from **1**(α) or **2**(α-1) by molecular weight (662.6) or molecular formula, its structure was readily elucidated from characteristic NMR signals leading to its structure assignment as shown in Fig. 6. It is important to note that **6**(ο) is not stable under acidic conditions, as dissolution in $CDCl_3$ (to record NMR spectra—first recorded in MeOH-d_4) resulted in rapid degradation affording NG-015[3] and **16**. (A similar acid sensitivity has also been noted for **10** and **13**, yielding **9** (**11**) and **16**. For this reason, the methylesters could only be prepared by reacting with diazomethane (see Fig. 9). Unlike **1** and **2**, **6** is inactive as an antifungal (os-1 assay[10]) presumably due to its acyclic nature.

The structures of the 'linear' 15G256 polyesters (**7**–**11**) were deduced similarly from analytical data, primarily those obtained by mass spectrometry and NMR spectroscopy such as COSY, DEPT, HETCOR (HSQC) and HMBC and allowed unambiguous structure assignments as depicted in Figs. 2 and 8. Typically, the mass spectra of the linear polyesters revealed relatively abundant fragment ions that aided greatly in their structure assignments (see Fig. 10). In comparison, only molecular adduct ions were generally observed in the mass spectra of the cyclic lactides with virtually no fragmentation. The NMR spectra also suggested

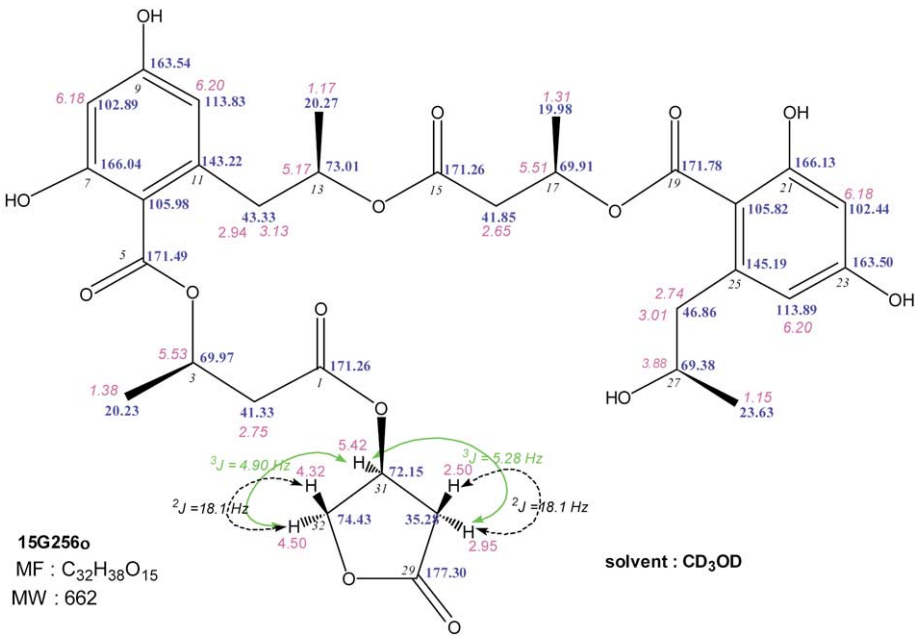

Figure 6. ^1H and ^{13}C NMR shift assignments for **6**(15G256ο).

Table 1. ^{13}C NMR shift values (ppm) of 15G256 polyester components in MeOH-d_4

Carbon #	Multiplicity	**1**(α)	**2**(α-1)	**7**(α-2)	**6**(ο)	**10**(π)	**8**(β-2)	**3**(β)	**4**(ι)	**5**(ω)
1	s	171.5	172.0	173.8	171.3	173.9	173.8	171.2	171.7	171.1
2	t	41.0	41.06	41.3	41.3	41.4	41.3	41.1	40.9	41.7
3	d	70.1	70.3	70.5	70.0	70.5	70.5	70.1	70.4	70.3
4	q	20.2	20.1	20.1	20.2	20.1	20.1	20.1	19.6	20.0
5	s	171.0	171.5	171.6	171.5	171.7	171.6	171.1	171.8	171.2
6	s	106.7	106.9	105.9	106.0	105.9	106.0	106.6	106.3	106.9
7	s	165.4	165.4	166.2	166.0	166.2	166.2	165.6	166.1	165.3
8	d	102.9	102.7	102.8	102.9	102.8	102.8	102.8	102.7	102.7
9	s	163.4	163.3	163.5	163.5	163.5	163.5	163.5	163.7	163.4
10	d	113.3	112.5	113.8	113.8	113.8	113.8	113.3	112.6	112.7
11	s	143.2	143.1	143.6	143.2	143.6	143.6	143.3	143.2	143.4
12	t	42.5	41.7	43.4	43.3	43.4	43.6	42.5	41.9	42.1
13	d	73.4	73.6	73.2	73.0	73.2	73.2	73.3	73.4	73.3
14	q	19.6	19.8	20.5	20.3	20.4	20.5	19.6	20.1	20.2
15	s	171.3	171.5	171.2	171.3	171.3	171.2	171.2		
16	t	41.6	41.5	41.8	41.9	41.8	41.8	41.5		
17	d	70.3	70.3	70.0	70.0	69.8	70.0	70.2		
18	q	20.2	20.1	19.9	20.0	19.9	19.9	20.2		
19	s	171.3	171.5	171.6	171. 8	171.8	171.6	171.3		
20	s	107.4	107.3	105.8	105.8	105.7	105.7	107.2		
21	s	165.0	165.0	166.2	166.1	166.2	166.3	165.1		
22	d	102.8	102.7	102.7	102.4	102.4	102.7	102.7		
23	s	163.3	163.4	163.5	163.5	163.5	163.5	163.3		
24	d	112.7	112.6	113.8	113.9	113.9	113.9	112.7		
25	s	143.1	143.1	143.7	145.2	145.2	143.8	143.0		
26	t	41.9	41.8	43.5	46.9	46.8	43.6	42.0		
27	d	73.9	73.6	72.8	69.4	69.4	72.7	73.9		
28	q	19.8	19.9	20.5	23.63	23.6	20.6	19.7		
29	s	171.4	171.7	172.7	177.3		172.6	171.4		
30	t	36.7	40.3	39.8	35.3		45.1	41.5		
31	d	72.7	67.1	69.7	72.2		65.4	69.1		
32	t(q)	63.6	68.5	66.4	74.7		22.9	19.9		

'ring-opened' forms of the polyesters with characteristic signals. A 'terminal' β-hydroxylbutyrate group was indicated by typical chemical shifts for two sets of proton signals at ca. 2.3 and 4 ppm, shifts that are observed at ca. 2.7 and 5.2 ppm when the compound is cyclic. Further, HMBC's from the methine proton (4.00 ppm) and the methylene protons (2.33 and 2.26 ppm) to only one carboxyl signal (172.6 ppm) corroborated the acyclic structures. Their ^{13}C and ^{1}H chemical shift values are compiled in Tables 1–4 together with those of the lactides. The numbering of the carbon and hydrogen atoms throughout the polyester chain, as shown in Figs. 1 and 2 for the polyesters was chosen to reflect their proposed biosynthesis. The indicated numbering system allows for an easy comparison of chemical shift values assigned to the respective subunits, but does not entirely agree with prevailing chemical nomenclature.

2.3. Absolute configuration

The absolute configurations of the polyesters were deduced from the negative rotation of two isolated constituents. The optical rotation of both, hydrolytically prepared (from **3**) and isolated **16** [6-hydroxymellein] gave $[\alpha]_D^{25}=-49.3\pm1$ (*c* 1.15%, MeOH) and the CD spectra (see Fig. 7) were identical to that previously published for this compound.[7] Therefore, **16** is (−)(*R*)-6-hydroxymellein, and not (*S*)-6-hydroxymellein which apparently is also known as a natural product.[8] The rotation of 3-hydroxy-butyrolactone, obtained from the degradation of **6**(ο), gave $[\alpha]_D^{25}=-75.3\pm1$ (*c* 0.82%, MeOH), indicating *S*-configuration.[9] Considering that (*S*)-3,4-dihydroxy-butyric acid is present in **1** as well as **2**, and 3-hydroxybutyric acid is the natural precursor, it can be deduced that, the absolute stereochemistry of the isolated polyesters is as indicated in Figs. 1, 2, 6 and 8.

2.4. Antifungal activity

The 15G256 polylactones inhibit the growth of a variety of phytopathogenic fungi.[2] Our in vitro tests using *Neurospora crassa* OS-1[10] (nikkomycin (MIC=2 μg/mL) as positive control) have demonstrated that **3**(β) is the most potent compound (MIC=0.5 μg/mL) of this series followed by **1**(α) and **2**(α-1) (MIC=2 μg/mL) whereas **4**(ι), and **5**(ω) are approximately 10-fold less active. The linear polyesters **6**(ο), **7**(α-2), **8**(β-2), **9**(ν) and **10**(π) do not inhibit fungal growth (cell wall biosynthesis).

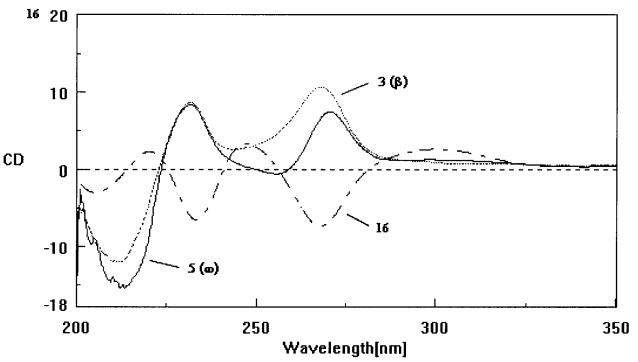

Figure 7. CD spectra of **3**, **5** and **16**.

Table 2. ^{13}C NMR shift values of 15G256 polyester components in MeOH-d_4

Carbon #	Multiplicity	**7**(α-2)	**12**(α-2me)	**8**(β-2)	**14**(β-2me)	**9**(*ν*)	**11**(*ν*-me)	**15**(*ν*-me2)
1	s	173.8	172.4	173.8	172.4	173.9	172.4	172.4
2	t	41.3	41.3	41.3	41.2	41.4	41.3	41.2
3	d	70.5	70.1	70.5	70.3	70.5	70.3	70.4
4	q	20.1	20.1	20.1	20.1	20.1	20.1	20.1
5	s	171.6	171.6	171.6	171.6	171.6	171.6	171.5
6	s	105.9	105.9	105.9	105.9	105.9	106.2	107.4
7	s	166.2	166.2	166.2	166.2	166.1	166.0	165.0
8	d	102.8	102.8	102.8	102.8	102.7	102.8	100.7
9	s	163.5	163.5	163.5	163.5	163.4	163.6	165.8
10	d	113.8	113.8	113.8	113.8	113.8	113.8	112.9
11	s	143.6	143.6	143.6	143.6	143.7	143.5	143.1
12	t	43.4	43.3	43.6	43.3	43.4	43.3	43.2
13	d	73.2	73.2	73.2	72.6	73.7	72.7	72.6
14	q	20.5	20.5	20.5	20.5	20.5	20.5	20.5
15	s	171.2	171.2	171.2	171.2	172.6	172.6	172.6
16	t	41.8	41.91	41.8	41.8	45.1	45.2	45.1
17	d	70.0	69.9	70.0	70.0	65.4	65.4	65.4
18	q	19.9	20.0	19.9	19.9	22.9	23.0	23.0
19	s	171.6	171.6	171.6	171.6			
20	s	105.8	105.8	105.7	105.7			
21	s	166.2	166.3	166.3	166.4			
22	d	102.7	102.7	102.7	102.7			
23	s	163.5	163.5	163.5	163.5			
24	d	113.8	113.8	113.9	113.9			
25	s	143.7	143.8	143.8	143.8			
26	t	43.5	43.6	43.6	43.6			
27	d	72.8	72.9	72.7	72.7			
28	q	20.5	20.5	20.6	20.6			
29	s	172.7	172.7	172.6	172.6			
30	t	39.8	39.9	45.1	45.1			
31	d	69.9	69.9	65.4	65.4			
32	t (q)	66.4	66.5	22.9	22.9			
1-OMe			52.3		52.3		52.3	52.3
9-OMe								55.9

Table 3. ^{1}H NMR shift values (ppm) of 15G256 polyester components recorded in MeOH-d_4

Proton[a] #	Multiplicity	**1**(α)	**2**(α-1)	**7**(α-2)	**6**(ο)	**10**(π)	**8**(β-2)	**3**(β)	**5**(ω)	**4**(ι)	**16**
2a	m	2.85	2.84	2.72	2.75	2.72	2.72	2.80	2.63	2.74	
2b	m	2.73	2.76	2.72	2.75	2.72	2.72	2.64	2.77	2.74	
3	m	5.53	5.56	5.55	5.53	5.55	5.55	5.51	5.49	5.53	
4	d	1.42	1.42	1.42	1.38	1.42	1.42	1.40	1.34	1.39	
8	d	6.23	6.19	6.19	6.18	6.19	6.19	6.21	6.19	6.19	6.19
10	d	6.24	6.23	6.21	6.20	6.21	6.21	6.23	6.23	6.22	6.21
12a	m	3.42	3.41	3.23	3.13	3.26	3.26	3.46	3.18	3.51	2.90
12b	m	2.79	2.89	2.86	2.94	2.86	2.87	2.75	3.00	2.83	2.81
13	m	5.01	5.04	5.19	5.17	5.19	5.19	5.01	5.16	5.08	4.64
14	d	1.12	1.17	1.23	1.17	1.22	1.22	1.12	1.19	1.18	1.45
16a	m	2.80	2.83	2.65	2.65	2.67	2.64	2.82			
16b	d	2.68	2.69	2.65	2.65	2.63	2.64	2.68			
17	m	5.50	5.45	5.52	5.51	5.50	5.51	5.49			
18	d	1.39	1.37	1.31	1.31	1.19	1.32	1.40			
22	d	6.20	6.20	6.19	6.18	6.19	6.19	6.20			
24	d	6.25	6.24	6.19	6.20	6.19	6.18	6.24			
26a	m	3.34	3.34	3.17	3.01	2.99	3.18	3.36			
26b	m	2.93	2.93	2.80	2.74	2.74	2.75	2.90			
27	m	5.03	5.10	5.16	3.88	3.88	5.15	5.02			
28	d	1.16	1.20	1.23	1.21	1.23	1.23	1.16			
30a	m	2.62	2.45	2.30	2.50		2.33	2.56			
30b	m	2.62	2.45	2.44	2.95		2.26	2.56			
31	m	5.25	4.16	3.96	5.42		4.00	5.25			
32	m	3.61	4.07	3.41	4.32		1.04	1.24			
(32b)	m				4.50						

[a] Proton chemical shifts were determined from 2D NMR spectra.

Table 4. ^{1}H NMR shift values (ppm) of 15G256 polyester components recorded in MeOH-d_4

Proton[a] #	Multiplicity	**7**(α-2)	**12**(α-2me)	**8**(β-2)	**14**(β-2me)	**9**(ν)	**11**(ν-me)	**15**(ν-me2)
2a	m	2.72	2.75	2.72	2.76	2.78	2.78	2.78
2b	m	2.72	2.76	2.72	2.74	2.76	2.76	2.76
3	m	5.55	5.55	5.55	5.57	5.57	5.57	5.58
4	d	1.42	1.40	1.42	1.43	1.44	1.44	1.44
8	d	6.19	6.19	6.19	6.21	6.20	6.20	6.35
10	d	6.21	6.21	6.21	6.22	6.20	6.20	6.32
12a	m	3.23	3.16	3.26	3.21	3.28	3.23	3.24
12b	m	2.86	2.92	2.87	2.89	2.87	2.89	2.92
13	m	5.19	5.18	5.19	5.19	5.20	5.19	5.19
14	d	1.23	1.20	1.22	1.23	1.28	1.27	1.27
16a	m	2.65	2.65	2.64	2.57	2.37	2.37	2.37
16b	d	2.65	2.65	2.64	2.64	2.27	2.27	2.27
17	m	5.52	5.52	5.51	5.51	4.03	4.03	4.01
18	d	1.31	1.33	1.32	1.32	1.06	1.07	1.04
22	d	6.19	6.19	6.19	6.19			
24	d	6.19	6.19	6.18	6.18			
26a	m	3.17	3.21	3.18	3.18			
26b	m	2.80	2.78	2.75	2.75			
27	m	5.16	5.16	5.15	5.15			
28	d	1.23	1.23	1.23	1.23			
30a	m	2.30	2.27	2.33	2.34			
30b	m	2.44	2.45	2.26	2.25			
31	m	3.96	3.93	4.00	4.01			
32	m	3.41	4.31	1.04	1.04			
1-OMe	s		3.67		3.67		3.67	3.67
								3.78

[a] Proton chemical shifts were determined from 2D NMR spectra.

2.5. Biogenesis

The structures of the acyclic compounds **7**(α-2), **8**(β-2), **9**(ν) and **10**(π) suggest that these compounds are biosynthetic precursors of the principal lactides **1**(α), **2**(α-1), and **3**(β), as well as **4**(ι), and **5**(ω). Although a study of the biosynthesis of any of the known macrocyclic polyesters has not been reported, it is envisioned that the biosynthesis of these macrocyclic esters follows a pattern similar to that employed in the synthesis of cyclic peptides. The assembly of the 15G256 lactides is apparently affected by alternately linking a β-hydroxybutyrate (**17**) and a 3,5-dihydroxy-7-(β-hydroxy-propyl)-benzoate [6-hydroxymellein (**16**)] moiety to form the polyesters (Fig. 8). The penultimate product of the propagating ester chain is **10**(π) which could undergo ring closure to yield **4**(ι), or receive a final attachment of β-hydroxybutyrate to generate the ultimate lactide precursor **8**(β-2). Currently, we assume that this last-attached β-hydroxybutyrate moiety of **8**(β-2) is enzymatically hydroxylated to give **7**(α-2) But it is conceivable that a preformed 3,4-dihydroxybutyrate unit can be coupled to **10**(π) as well. However, the selectivity with which this sequential coupling (esterification) process occurs would suggest that *H. oceanicum* uses the first proposed mechanism. Product profiles obtained from various fermentations at selected time points suggest that the 'hydroxylation reaction' is strongly dependent on environmental conditions. In fermentations with high titers the production of **3**(β) is predominant accompanied by low yields of **1**(α) or **2**, whereas in low titer productions **1**(α) may be the predominant lactide. It is apparent that **7**(α-2) and **8**(β-2) are the immediate precursors for **1**(α), **2**α and **3**(β), respectively, as suggested in Fig. 8. Polyester **8**(β-2)would be converted predominantly to **3**(β) but could still serve as precursor of other products. Lactide **4**(ι) might still be formed under loss of β-hydroxybutyric acid, while insertion of another 3,5-dihydroxy-7-(β-hydroxypropyl)-benzoate (**16**) would afford trimer **5**(ω).

3. Conclusion

The elucidated structures of the various 15G256 components reveal that **1**, originally the predominant antifungal component produced by culture LL-15G256, is identical with the two recently reported natural products BK223-A[2] and NG-012.[3] Compound **2** is indistinguishable from BK223-B[2] and NG-011,[3] while **3** matches the characteristics of BK223-C[2] and F26263,[4] including orbuticin.[5] Reportedly, the producing fungi, *Penicillium verruculosum*,[2,3] *Scedosporium apiospermum*,[4] and *Acremonium butyri*[5] are of terrestrial origin. Our report is the first to denote production of these and other lactides (**4**, **5**) as well as their biosynthetic precursors (**7**–**10**) by the marine fungus, *H. oceanicum*. Correlation of the newly described structures suggests a plausible biosynthetic pathway towards the macrocyclic polyesters (lactides **1**–**5**). The 15G256 polyesters may be formed by linking the respective hydroxy-acids to first yield polyesters and eventually the macrocyclic lactides in an enzymatic process similar to that used for the biosynthesis of macrocyclic peptides. Naturally occurring polyesters are rare and only recently true macrocyclic polyesters such as the macrosphelides have been reported.[11] Previously, only members of the nonactin family (tetronolides) could be considered macrocyclic polyester antibiotics.[12] Unlike the nonactins, the 15G256 lactides are virtually inactive as antibacterial agents. The exact molecular mechanism of their antifungal activity has not been established yet. However, since the acyclic 15G256 components are inactive, it is obvious

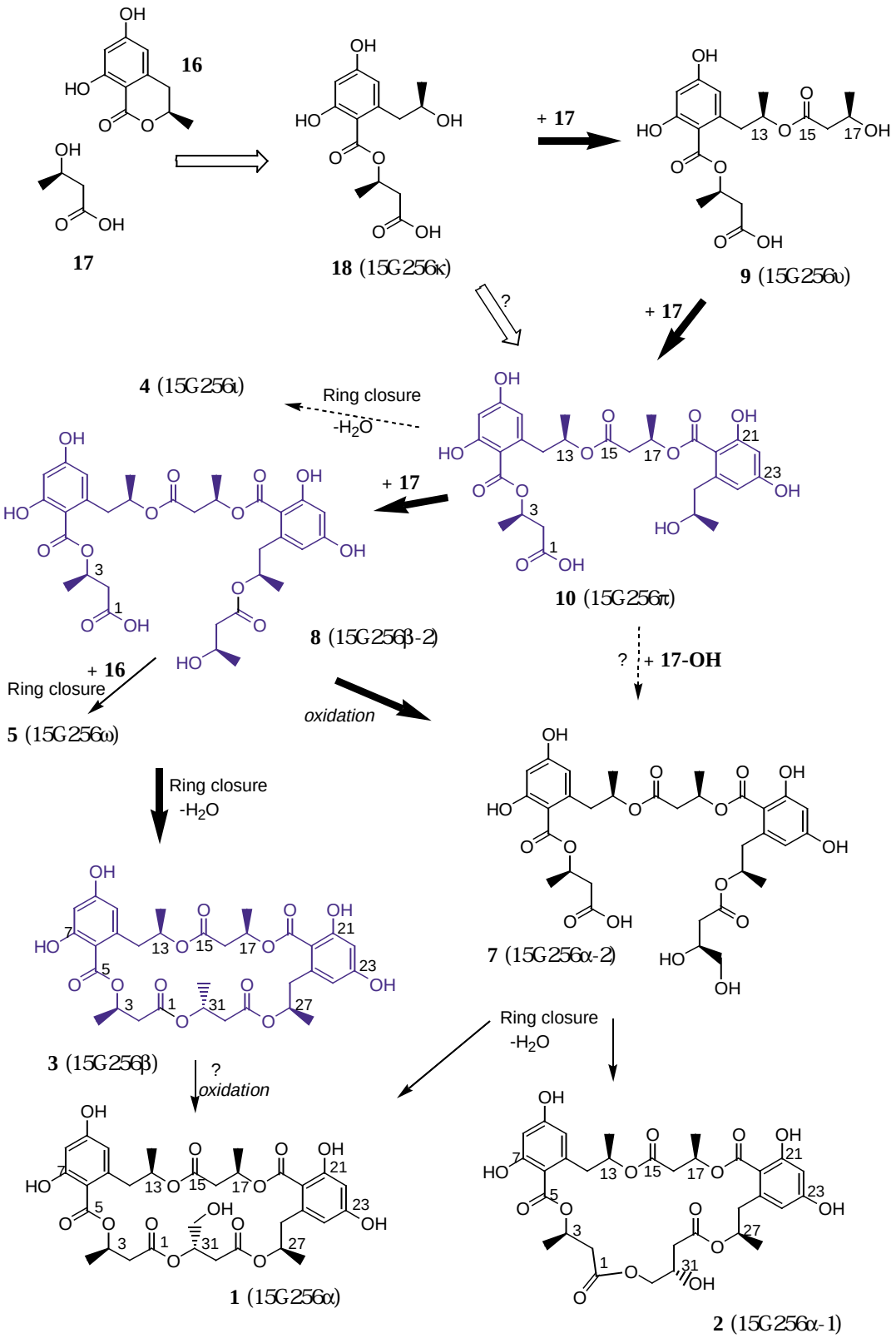

Figure 8. Proposed biosynthesis of the 15G256 macrolides.

that a ring structure is a mandatory requirement for activity.

A chemical synthesis of 15G256 polyester derivatives with different ring sizes would be desirable for the evaluation of a structure–activity relationship. Although the macrosphelides as well as the nonactins were synthesized,[11,12] the chemical synthesis of the 15G256 lactides may be a more challenging endeavor due to their increased hydrophilicity and acidic nature of the mellein moiety.

4. Experimental

4.1. General

A Hewlett-Packard 1100 or 1090M LC system with diode array detection (monitored at 262 nm) employing a variety of columns was used for the analysis of fractions or to check the purity of isolated components. Columns (either a RAININ Microsorb (C-18), a Whatman Partisil 5 C_8 reverse phase column (5 μm, 4.6×100 mm^2), or a Supelcosil LC-ABZ (5 μm, 4.6×150 mm^2) column) were all eluted isocratically with either 70% MeOH/20% H_2O/10% 0.1 M TFA, or 55% MeCN/20% H_2O/10% 0.1 M TFA at a flow rate of 1 mL/min (compare Table 5 for retention times). Samples were frequently analyzed by LC/MS using a model HP1100 LC system with tandem photodiode array and mass spectral detection. Compounds were resolved on a YMC ODS-A (4.6×150 mm^2) C18 HPLC column using linear gradient from 50 to 90% mobile phase B (0.025% formic acid (FA) in MeOH (or MeCN)) in mobile phase A (0.025% FA in water) over 30 min. The flow rate was 0.8 mL/min (see Table 5). A total scan UV chromatogram was acquired over a scan range from 190 to 400 nm with UV spectra acquired throughout the run from 190 to 400 nm at scan steps of 2 nm. After emerging from the UV flow cell, the effluent stream was split 3:1 with a flow of 0.2 mL/min. going to a Finnigan LCQ ion trap mass spectrometer and the remainder going to waste. The mass spectrometer is fitted with an electrospray ionization (ESI) probe and operated in alternating positive-ion and negative-ion full scan (100–2000 mass units) mode. The spray needle voltage was set to 6 kV for positive and 4.5 kV for negative. The capillary voltages were set at 29 and −10 for positive and negative, respectively. The capillary temperature was set to 200°C, and nitrogen was used as the sheath and auxiliary gasses which were set to 60 and 25 units, respectively.

HRFAB mass spectra were recorded using a VG-ZAB SE high performance mass spectrometer and a VG-11-230 data system.

Preparative HPLC separations were accomplished on a Whatman CCS/C_8 column (2×50 cm) or a MODCol® Kromasil C_{18} column (2.54×25 cm) using either 72% MeOH/water or 50% MeCN/water (when indicated 0.5 mL TFA/liter of solvent was added), with a flow rate of 9.9 mL/min and monitored by a variable wavelength detector (LDC) at 280 nm (see Fig. 3 or Fig. 4). Solvent was delivered with a Waters 600 MS HPLC pump. For larger preparations a RAININ Dynamax® C_{18} cartridge column system (5×50 cm) was used with a flow rate of 40 mL/min and monitored by a Model UV-1 variable wavelength detector (RAININ) at 280 nm.

Silica gel chromatography was performed on self-packed open columns by step gradient elution using methylene chloride/ethyl acetate mixtures followed by washes with methanol. Fractions from all columns were generally collected by hand and pooled according to peaks observed on TLC or HPLC analysis. All solvents were obtained from J. T. Baker, Inc., and were of the highest commercially available purity.

Solutions of pure compounds were concentrated by evaporation under reduced pressure and the material was subsequently obtained as an amorphous solid by freeze-drying from *t*-BuOH solutions.

IR spectra were obtained with a Nicolet 20XAB FT-IR spectrometer.

NMR spectra were obtained on a Bruker AMX 300 or 400 MHz NMR instrument. Chemical shifts are given in ppm relative to the solvent signals of DMSO-d_6 at δ 2.49 ppm (^{1}H) and δ 39.50 ppm (^{13}C), acetone-d_6 at δ 2.04 ppm (^{1}H) and δ 29.80 ppm (^{13}C), $CDCl_3$ at δ 7.26 ppm (^{1}H) and δ 77.0 ppm (^{13}C), or MeOH-d_4 at δ 3.30 ppm (^{1}H) and δ 49.00 ppm (^{13}C), respectively.

CD spectra were obtained in MeOH on a JASCO 715 spectropolarimeter using a 2x1 cm cell with concentrations of 15 μmol/L at 22°C (compare Fig. 7).

Table 5. HPLC retention times of various 15G256 components

Compound	C_{18} MeOH[a]	C_{18} MeCN[b]	C_8 MeOH[c]	C_{18} MeCN[d]
18	4.5	3.1		
16	6.0	4.0	2.9	5.1
9(ν)	7.1	3.4	3.2	4.0
11(ν-me)	10.6			
7(α-2)	14.2	3.4	6.25	4.9
10(π)	14.1	3.9	6.3	5.9
13(π-me)	16.6			
8(β-2)	17.2	4.3	9.7	7.3
12(α-2-me)	18.7			
6(ο)				8.8
1(α)	19.4	5.5	10.8	9.2
2(α-1)	21.0	5.8	12.6	10.0
14(β-2-me)	21.8			
4(ι)	22.2	8.62		
3(β)	22.7	10.57	**28.4**	
5(ω)	25.8	11.52		

[a] Gradient elution with MeOH (50–90% over 30 min) and 0.025% formic acid—column: YMC ODS AQ (10.0×0.46 cm, 5 μm).
[b] Isocratic elution with 55% acetonitrile and 0.05 M TFA—column: RAININ Microsorb C-18 (5 μm, 25×0.46 cm).
[c] Isocratic elution with 55% MeOH and 0.05 M TFA—column: Whatman C_8 cartridge (12.5×0.46 cm, 5 μm).
[d] Isocratic elution with 55% acetonitrile and 0.05 M TFA—column: RAININ Microsorb C-18 (5 μm, 25×0.46 cm).

4.2. Isolation and purification of the 15G256 components 15G256α (1), α-1 (2) and β (3)

Whole mash (5 L) was separated into pellet and supernatant by centrifugation at 3000 rpm for 30 min. The pellet was extracted with 2 L of 85% aqueous acetone while the supernatant was extracted with 2 L of ethyl acetate. The organic extract of the supernatant and the pellet extract were processed separately under the following conditions. After evaporation of the solvent, the remaining solids (ca. 2 g from the pellet and ca. 1.2 g from the supernatant) were re-suspended in methylene chloride and loaded onto a self-packed silica gel column (21×300 mm^2). The compounds were eluted with increasing concentrations of ethyl acetate (10, 25, 50, and 100%) followed by a final column wash with 100% MeOH.

Silica gel fractions, as listed in Table 6 were obtained from

Table 6. Silica gel fractions

Fraction	Amount (mg)	Solvent	Compound	Comment
A	64.1	100% CH_2Cl_2	Oily	(Discarded)
B	550	10–25% EtOAc	**3**–**5**	Fractions separated further by prep RP-HPLC
C	470	25–50% EtOAc	**1**–**3**, **6**	
D and E	43.5	50–100% EtOAc	15G-γ,δ,ε	
F	250	100% MeOH	**7**–**10**	
A1	33	100% CH_2Cl_2	Oily	(Discarded)
B1	114	10–25% EtOAc	**3** (~pure)	Fractions separated further by prep RP-HPLC
C1	423	25–50% EtOAc	**1**–**3**, **6**	
D1	125	50–100% EtOAc	**1**, **2**, **6**	
E1	52	100% EtOAc	15G-γ,δ,ε	
F1	476	100% MeOH	**7**–**10**	

the supernatant extract (A–F) as well as from the pellet extract (A1–F1), and were subsequently subjected to reverse phase chromatography under the conditions described above.

Finally, after pooling the appropriate fractions, 15G256α (420 mg), 15G256α-1 (380 mg), and 15G256β (560 mg) gamma were recovered as freeze-dried, off-white powders. Yields of other pure components: **16** (22 mg), 15G256ν (38 mg), 15G256α-2 (63 mg), 15G256β-2 (94 mg) and 15G256π (26 mg).

4.3. Preparation of methyl esters 11 (15), 12, 13 or 14

Dry **7**–**9** or **10** (5 mg) was dissolved in 5 mL methanol and an etheral solution of CH_2N_2 (1%) was slowly added while swirling the reagent vessel. The reaction was followed by HPLC analysis using an analytical Supelcosil LC-ABZ C_{18} reverse phase column eluted with 70% MeOH/10% 0.1 M TFA/20% water. Generally, the chromatogram revealed that the original peak for the respective 15G256 component had disappeared and new, more retaining peak was observed instead. When the reaction was complete, the solvent was evaporated in a stream of nitrogen. Analysis of the dried products showed the presence of the respective methyl ester (**7** yields **12**, **8** affords **14**, **9** turned to **11**, and**10** provided **13**; compare Tables 2, 4, and 5).

Our first methylation of **9** was carried out in CH_2Cl_2 and yielded two products, **11** and **15** that were separated by TLC. When the same reaction was carried out in MeOH, **11** was formed almost exclusively.

4.4. Physico-chemical properties of isolated polyesters

4.4.1. 15G256α (1). $C_{32}H_{38}O_{15}$ MW 662.64 (see Fig. 8) IR (KBr) 3417, 2981, 2853 (s), 2671, 1733 (s), 1649 (s), 1621 (s), 1452, 1383, 1353, 1314, 1260, 1191, 1140, 1099, 1053 cm^{-1}; UV (MeOH) λ_{max} nm (ε) 216 (40,800), 264 (22,460), 302 (9760); CD (MeOH) λ_{ext} nm ($\Delta\varepsilon$) 211.8 (−11.85), 231.6 (8.98), 268.6 (10.10, (rel. val.)); $[\alpha]_D^{25}=-24.4\pm1$ (*c* 1.15%, MeOH); ^1H NMR (see Table 3); ^{13}C NMR (see Table 1); MS (FAB) $[M+H]^+=m/z$ 663.4; MS (FAB) $[M+Na]^+=m/z$ 685.4; LC/MS-ESI: $[M+H]^+=m/z$ 663.0 (100%), $[M+Na]^+=m/z$ 685.1, $[M+NH_4]^+=m/z$ 680.9, small frag.: 645.1, 569.1, 469.1, 383.1, 365.1, 281.1, 195.2 (20%), 177.1.

4.4.2. 15G256α-1 (2). $C_{32}H_{38}O_{15}$ MW 662.64 (see Fig. 1) UV (MeOH) λ_{max} nm (ε) 216 (40,800), 264 (22,460), 302 (9760); CD (MeOH) λ_{ext} nm ($\Delta\varepsilon$) 212.4 (−14.02), 231.0 (8.41), 268.6 (10.43, (rel. val.)); ^1H NMR (see Table 3); ^{13}C NMR (see Table 1); MS (FAB) $[M+H]^+=m/z$ 663.4; MS (FAB) $[M+Na]^+=m/z$ 685.4; LC/MS-ESI: $[M+H]^+=m/z$ 663.0 (100%), $[M+Na]^+=m/z$ 685.1, $[M+NH_4]^+=m/z$ 680.9, small frag.: 645.1, 569.1, 469.1, 383.1, 281.1, 195.2 (20%), 177.1.

4.4.3. 15G256β (3). $C_{32}H_{38}O_{14}$ MW 646.64 (see Fig. 1) UV (MeOH) λ_{max} nm (ε) 216 (45,330), 264 (22,870), 302 (10,000); CD (MeOH) λ_{ext} nm ($\Delta\varepsilon$) 212.2 (−12.02), 231.6 (8.53), 268.6 (10.50, (rel. val.)) (see Fig. 7); $[\alpha]_D^{25}=-24.7\pm1$ (*c* 1.25%, MeOH); ^1H NMR (see Table 3); ^{13}C NMR (see Table 1); MS (FAB) $[M+H]^+=m/z$ 647.4; MS (FAB) $[M+Na]^+=m/z$ 669.4.

4.4.4. 15G256ι (4). $C_{28}H_{32}O_{12}$ MW 560.55 (see Fig. 1) crystalline, mp 156°C UV (MeOH) λ_{max} nm (ε) 216 (46,420), 264 (23,420), 302 (10,240); CD (MeOH) λ_{ext} (nm)/$\Delta\varepsilon$=215.6 (−10.38), 232.2 (10.41), 256.6 (−6.95), 271.2 (3.37), 304.4 (3.22, (rel. val.)); ^1H NMR (see Table 3); ^{13}C NMR (see Table 1); HRFABMS $[M+Na]^+=m/z$ 583.1784, calcd for $C_{28}H_{32}O_{12}Na$=583.1777 (Δ=−0.7 mmu); MS (FAB) $[M+H]^+=m/z$ 561.2; MS (FAB) $[M+Na]^+=m/z$ 583.3; LC/MS-ESI: $[M+H]^+=m/z$ 561.0 (100%), $[M+Na]^+=m/z$ 583.2, $[M+NH_4]^+=m/z$ 578.9, small frag.: 489.1, 367.1, 281.1, 195.2 (40%), 177.1.

4.4.5. 15G256ω (5). $C_{42}H_{48}O_{18}$ MW 840.82 (see Fig. 1) UV (MeOH) λ_{max} nm (ε) 216 (62,000), 264 (34,100), 302 (14,820); CD (MeOH) λ_{ext} nm ($\Delta\varepsilon$) 213.6 (−15.5), 231.8 (8.20), 255.8 (−0.72), 271.0 (7.27), 302.2 (1.07, (rel. val.)) (see Fig. 7); ^1H NMR (see Table 3); ^{13}C NMR (see Table 1); HRESMS $[M+H]^+=m/z$ 841.29114, calcd for $C_{42}H_{49}O_{18}$=481.29134 (Δ=−0.2 mmu); MS (FAB) $[M+H]^+=m/z$ 841.5; MS (FAB) $[M+Na]^+=m/z$ 863.5; LC/MS-ESI: $[M+H]^+=m/z$ 841.0 (100%), $[M+Na]^+=m/z$ 863.1, $[M+NH_4]^+=m/z$ 857.9, small frag.: 585.4, 489.1, 438.6, 281.1, 195.2.

4.4.6. 15G256ο (6). $C_{32}H_{38}O_{15}$ MW 662.64 (see Fig. 6) UV (MeOH) λ_{max} nm (ε) 216 (40,800), 264 (22,460), 302 (9760); ^1H NMR (see Table 3); ^{13}C NMR (see Table 1); LC/MS-ESI: $[M+H]^+=m/z$ 662.9 (100%), $[M+Na]^+=m/z$ 685.2, $[M+NH_4]^+=m/z$ 681.0, frag.: 645.0, 577.1, 451.1, 365.0 (100%), 281.1, 195.1 (80%), 171.1.

4.4.7. 15G256α-2 (7). $C_{32}H_{40}O_{16}$ MW 680.64 (see Fig. 2)

UV (MeOH) λ_{max} nm (ε) 216 (40,800), 264 (22,460), 302 (9760); ^{1}H NMR (see Table 3); ^{13}C NMR (see Table 1); MS (FAB) [M−dihydroxybutyrate]$^+$=*m/z* 651.3; MS (FAB) [M+Na]$^+$=*m/z* 703.2; LC/MS-ESI: [M]$^+$=*m/z* 680.6, [M+NH$_4$]$^+$=*m/z* 697.9, frag.: 577.0, 561.0 (100%), 367.0, 281.0 (50%), 195.1 (50%), 177.1.

4.4.8. 15G256β-2 (8). $C_{32}H_{40}O_{15}$ MW 664.65 (see Fig. 2) UV (MeOH) λ_{max} nm (ε) 216 (40,800), 264 (22,460), 302 (9760); ^{1}H NMR (see Table 3); ^{13}C NMR (see Table 1); MS (FAB) [M+H]$^+$=*m/z* 665.3; MS (FAB) [M+Na]$^+$=*m/z* 687.2; LC/MS-ESI: [M]$^+$=*m/z* 664.6 (50%), [M+NH$_4$]$^+$=*m/z* 681.9, frag.: 561.0 (100%), 367.0, 281.0 (50%), 195.1 (45%), 177.1 (see Fig. 10).

4.4.9. 15G256*ν* (9). $C_{18}H_{24}O_9$ MW 384.38 (see Fig. 2) UV (MeOH) λ_{max} nm (ε) 216 (22,390), 264 (11,300), 302 (4940); ^{1}H NMR (see Table 4); ^{13}C NMR (see Table 2); MS (FAB) [M+Na]$^+$=*m/z* 407.2; [M+Na−H$_2$O]$^+$=*m/z* 389.3; [M+H−hydroxybutyrate]$^+$=*m/z* 281.1; LC/MS-ESI: [M+H]$^+$=*m/z* 385.0, [M+Na]$^+$=*m/z* 407.1, [M+NH$_4$]$^+$=*m/z* 402.0, frag.: 281.0 (100%), 195.2 (40%), 177.1.

4.4.10. 15G256π (10). $C_{28}H_{34}O_{13}$ MW 578.56 (see Fig. 2) UV (MeOH) λ_{max} nm (ε) 216 (46,420), 264 (23,420), 302 (10,240); ^{1}H NMR (see Table 3); ^{13}C NMR (see Table 1); MS (FAB) [M+H]$^+$=*m/z* 579.3; MS (FAB) [M+Na]$^+$=*m/z* 601.2; LC/MS-ESI: [M]$^+$=*m/z* 578.8 (100%), [M+Na]$^+$=*m/z* 601.1, [M+NH$_4$]$^+$=*m/z* 596.0, frag.: 561.1, 281.1 (80%), 195.1 (60%), 177.1.

4.4.11. 11 (15G256*ν*-me). $C_{19}H_{26}O_9$ MW 398.40 (see Fig. 9) UV (MeOH) λ_{max} nm (ε) 216 (22,390), 264 (11,300), 302 (4940); ^{1}H NMR (see Table 4); ^{13}C NMR (see Table 2); MS (FAB) [M+Na]$^+$=*m/z* 407.2; [M+Na−H$_2$O]$^+$=*m/z* 389.3; [M+H−hydroxybutyrate]$^+$=*m/z* 281.1 LC/MS-ESI: [M+H]$^+$=*m/z* 399.0, [M+Na]$^+$=*m/z* 421.4, [M+NH$_4$]$^+$=*m/z* 416.0, frag.: 295.0 (80%), 195.1 (100%), 177.1.

4.4.12. 12 (15G256α-2-me). $C_{33}H_{42}O_{16}$ MW 694.64 (see Fig. 10) UV (MeOH) λ_{max} nm (ε) 216 (40,800), 264 (22,460), 302 (9760); ^{1}H NMR (see Table 4); ^{13}C NMR (see Table 2); LC/MS-ESI: [M]$^+$=*m/z* 694.6 (40%),

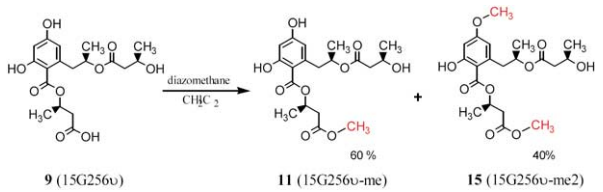

Figure 9. Methylation of **9**.

[M+NH$_4$]$^+$=*m/z* 711.9, frag.: 575.0 (100%), 381.0, 295.0 (25%),195.1 (30%), 177.1 (see Fig. 10).

4.4.13. 13 (15G256π-me). $C_{29}H_{36}O_{13}$ MW 592.59 UV (MeOH) λ_{max} nm (ε) 216 (46,420), 264 (23,420), 302 (10,240); LC/MS-ESI: [M−H]$^+$=*m/z* 592.8 (100%), [M+Na]$^+$=*m/z* 615.1, [M+NH$_4$]$^+$=*m/z* 609.9, frag.: 574.9, 295.0 (100%), 195.1 (80%), 177.1.

4.4.14. 14 (15G256β-2-me). $C_{33}H_{42}O_{15}$ MW 678.68 UV (MeOH) λ_{max} nm (ε) 216 (40,800), 264 (22,460), 302 (9760); ^{1}H NMR (see Table 4); ^{13}C NMR (see Table 2); LC/MS-ESI: [M+H]$^+$=*m/z* 678.5 (45%), [M+NH$_4$]$^+$=*m/z* 696.0, frag.: 575.0 (100%), 561.0 (40%), 381.0, 295.0 (40%), 281.1, 195.1 (45%), 177.1.

4.4.15. 15 (15G256*ν*-me2). $C_{20}H_{28}O_9$ MW 412.43 (see Fig. 9) UV (MeOH) λ_{max} nm (ε) 216 (22,390), 264 (11,300), 302 (4940); ^{1}H NMR (see Table 4); ^{13}C NMR (see Table 2); LC/MS-ESI: [M+H]$^+$=*m/z* 413.1, [M+NH$_4$]$^+$=*m/z* 430.2, frag.: 309.1 (75%), 208.1 (100%), 177.1.

4.4.16. (*R*)-6-Hydroxymellein (16). $C_{10}H_{10}O_4$ MW194.18 [(3*R*)3,4-Dihydro-6,8-dihydroxy-3-methylisocoumarin] (15G256-P2) (see Fig. 8) UV (MeOH) λ_{max} nm (ε) 216 (18,910), 268 (12,500), 300 (5100); CD (MeOH) λ_{ext} nm ($\Delta\varepsilon$) 219.6 (2.34), 233.6 (−7.28), 247.4 (3.09), 268.2 (−7.61), 301.6 (2.48, (rel. val.)) (see Fig. 7) $[\alpha]_D^{25}$=−49.3±1 (*c* 1.15%, MeOH); ^{1}H NMR (see also Table 3): 6.19 (s, H-8), 6.21 (s, H-10), 4.64 (m, *J*=3.5, 10.9, 6.3 Hz, H-13), 2.90 (dd, *J*=3.5, 16.4 Hz, H-12a), 2.81 (dd, *J*=10.9, 16.4 Hz, H-12b), 1.45 (d, *J*=6.3 Hz, H$_3$-14) ^{13}C NMR(CD$_3$OD): 171.69 (C-5), 101.47 (C-6), 166.26 (C-7),

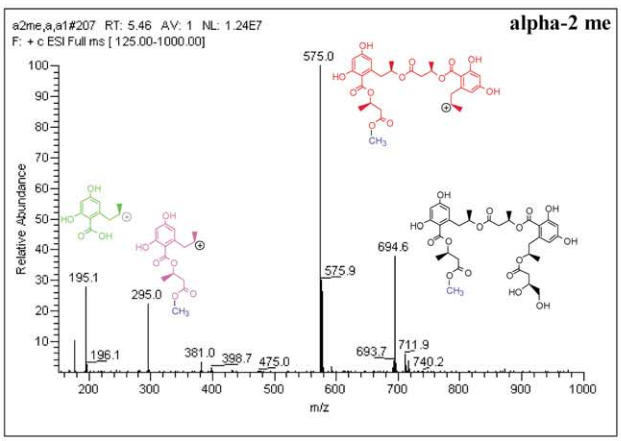

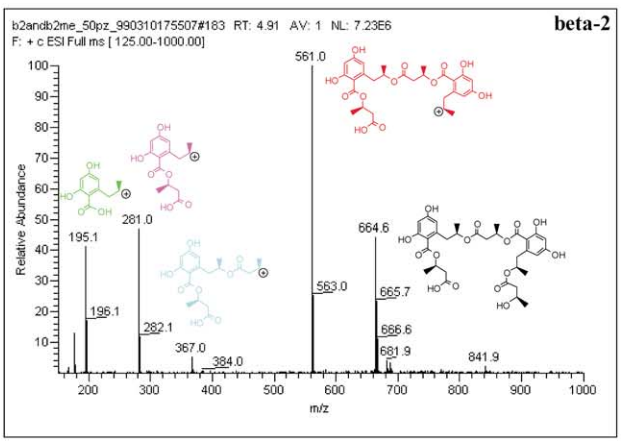

Figure 10. ESI/MS spectra of **12**(α-2-me) and **8**(β-2).

102.17 (C-8), 165.63 (C-9), 107.85 (C-10), 143.50 (C-11), 35.51 (C-12), 77.18 (C-13), 20.83 (C-14); MS (FAB) $[M+H]^+=m/z$ 195.2; LC/MS-ESI: $[M+H]^+=m/z$ 195.1 (100%).

4.4.17. 18 (15G256κ). $C_{14}H_{18}O_7$ MW 298.28 (see Fig. 8) UV (MeOH) λ_{max} nm (ε) 216 (22,390), 264 (11,300), 302 (4940); LC/MS-ESI: $[M+H]^+=m/z$ 299.1, $[M+Na]^+=m/z$ 321.1, $[M+NH_4]^+=m/z$ 316.1, frag.: 281.0, 212.0, 195.1 (100%), 177.1.

Acknowledgments

We appreciate the determination of molecular weights (HRMS) by our colleague R. Tsao. We would also like to thank our friends at the former Cyanamid Agricultural Research Center and our co-workers in the Natural Products Section at Wyeth Research for their support in this program.

References

1. (a) Abbanat, D.; Leighton, M.; Maiese, W.; Jones, E. B. G.; Pearce, C. J.; Greenstein, M. *J. Antibiot.* **1998**, *51*(3), 296–302. (b) Schlingmann, G.; Milne, L.; Carter, G. T. *J. Antibiot.* **1998**, *51*(3), 303–316.
2. Breinholt, J.; Jensen, G. W.; Nielsen, R. I.; Olsen, C. E.; Frisvad, J. C. *J. Antibiot.* **1993**, *46*(7), 1101–1108.
3. Ito, M.; Maruhashi, M.; Sakai, N.; Mizoue, K.; Hanada, K. *J. Antibiot.* **1992**, *45*(10), 1559–1572.
4. Kondo, H.; Kurama, M.; Nakajima, S.; Osada, K.; Ookura, A.; Suda, H. Japanese Patent 1991 JP 05032658 A2 930209 Heisei. -JP 91-191061 91.07.05.
5. Roy, K.; Chatterjee, S.; Deshmunkh, S. K.; Vijayakumar, E. K. S.; Ganuli, B. N.; Fehlhaber, H. W. *J. Antibiot.* **1996**, *49*(11), 1186–1187.
6. Hamill, R. L.; Higgins, C. E.; Boaz, H. E.; Gorman, M. *Tetrahedron Lett.* **1969**, *49*, 4255–4258.
7. Krohn, K.; Bahramsari, R.; Florke, U.; Ludewig, K.; Kliche-Spory, C.; Michel, A.; Aust, H.-J.; Draeger, S.; Schulz, B.; Antus, S. *Phytochemistry* **1997**, *45*(2), 313–320.
8. (a) Biswas, K. M.; Mallik, H. *Phytochemistry* **1986**, *25*(7), 1727–1730. (b) Venkatasubbaiah, P.; Chilton, W. S. *J. Nat. Prod.* **1991**, *54*, 1293–1297.
9. Huang, G.; Hollingsworth, R. I. *Tetrahedron* **1998**, *54*(8), 1355–1360.
10. Kirsch, D. R.; Lai, M. H. *J. Antibiot.* **1986**, *39*, 1620–1622.
11. (a) Takamatsu, S.; Kim, Y.-P.; Hayashi, M.; Natori, M.; Komiyama, K.; Omura, S. *J. Antibiot.* **1997**, *50*, 878–880. (b) Fukami, A.; Taniguchi, Y.; Nakamura, T.; Rho, M.-C.; Kawaguchi, K.; Hayashi, M.; Komiyama, K.; Omura, S. *J. Antibiot.* **1999**, *52*(5), 501–504.
12. (a) Gerlach, H.; Oertle, K.; Thalmann, A.; Servi, S. *Helv. Chim. Acta* **1975**, *58*, 2036–2043. (b) Bartlett, P. A.; Meadows, J. D.; Ottow, E. *J. Am. Chem. Soc.* **1984**, *106*, 5304–5311.